

A mode coupling theory description of the short- and long-time dynamics of nematogens in the isotropic phase

Jie Li, Hu Cang, Hans C. Andersen, and M. D. Fayer^{a)}
Department of Chemistry, Stanford University, Stanford, California 94305

(Received 22 August 2005; accepted 31 October 2005; published online 3 January 2006)

Optical heterodyne-detected optical Kerr effect (OHD-OKE) experimental data are presented on nematogens 4-(trans-4'-n-octylcyclohexyl)isothiocyanatobenzene (8-CHBT), and 4-(4'-pentyl-cyclohexyl)-benzotrile (5-PCH) in the isotropic phase. The 8-CHBT and 5-PCH data and previously published data on 4'-pentyl-4-biphenylcarbonitrile (5-CB) are analyzed using a modification of a schematic mode coupling theory (MCT) that has been successful in describing the dynamics of supercooled liquids. At long time, the OHD-OKE data (orientational relaxation) are well described with the standard Landau-de Gennes (LdG) theory. The data decay as a single exponential. The decay time diverges as the isotropic to nematic phase transition is approached from above. Previously there has been no theory that can describe the complex dynamics that occur at times short compared to the LdG exponential decay. Earlier, it has been noted that the short-time nematogen dynamics, which consist of several power laws, have a functional form identical to that observed for the short time behavior of the orientational relaxation of supercooled liquids. The temperature-dependent orientational dynamics of supercooled liquids have recently been successfully described using a schematic mode coupling theory. The schematic MCT theory that fits the supercooled liquid data does not reproduce the nematogen data within experimental error. The similarities of the nematogen data to the supercooled liquid data are the motivation for applying a modification of the successful MCT theory to nematogen dynamics in the isotropic phase. The results presented below show that the new schematic MCT theory does an excellent job of reproducing the nematogen isotropic phase OHD-OKE data on all time scales and at all temperatures. © 2006 American Institute of Physics. [DOI: [10.1063/1.2145679](https://doi.org/10.1063/1.2145679)]

I. INTRODUCTION

The orientational relaxation dynamics of nematogens in the isotropic phase differ from those of conventional liquids but have been shown experimentally to be very similar to those of fragile supercooled liquids.¹ However, there are some significant differences between the dynamics of nematogens and fragile supercooled liquids because of the partial nematic ordering that exists in the isotropic phase of nematogens. Above but near the nematic-isotropic (NI) phase transition, nematogen orientational dynamics are strongly influenced by local structures (pseudonematic domains) that exist in the isotropic phase.^{2,3} Using both time and frequency domain methods, considerable experimental work has examined the relatively long time scale orientational relaxation that is associated with the randomization of the pseudonematic domains.⁴⁻¹² Near the NI phase transition, the isotropic phase is nematically ordered on a distance scale defined by a correlation length, ξ .^{2,3} As the NI phase transition is approached from above, ξ grows, becoming infinite in the nematic phase. On the time scales of many nanoseconds to hundreds of nanoseconds, depending on the temperature, the local order randomizes, giving rise to exponential decays of time domain optical Kerr effect experiments^{4,12}

The long-time-scale relaxation of the local structures is

described by Landau-de Gennes (LdG) theory, which was formulated to describe the NI phase transition and the dynamics and nematiclike local order above the phase transition.² The NI phase-transition is weakly first order, and it has a noticeable effect on properties of the liquid near the phase transition temperature, T_{NI} . LdG theory predicts the temperature dependence of the long-time exponential decay in the isotropic phase, which has a sharply increasing decay time as the transition temperature is approached. LdG theory has been confirmed many times experimentally using techniques such as optical Kerr effect,^{4,5,12} depolarized light scattering,⁶ dynamic light scattering,⁷ magnetic⁸ and electric birefringence,⁹ and dielectric relaxation^{10,11} The influence of the pseudonematic domains on the long time scale dynamics continues up to ~ 50 °K above the NI phase-transition temperature.¹² LdG theory gives the correlation length as

$$\xi(T) = \xi_0 [T^*/(T - T^*)]^{1/2}, \quad (1)$$

where ξ_0 is molecular length scale (typically 7–8 Å), and T^* is a temperature 0.5–1.0 K lower than T_{NI} .³ [The approach toward the critical temperature from above causes the apparent divergence of the relaxation time, but before T^* is reached a weakly first-order transition occurs at T_{NI} . Hence it is T^* rather than T_{NI} that appears in the denominator of Eq. (1).] At high temperatures, the size of the domains becomes similar to the molecular volume, and LdG theory ceases to apply.¹²

^{a)}Electronic mail: fayer@stanford.edu

On time scales short compared to the time for pseudone-matic domain randomization, and on distance scales short compared to ξ , nematogens exist in an environment with nematiclike order. Dynamics on short time scales (less than a few nanoseconds) are not described by the LdG theory. A number of studies have investigated orientational relaxation dynamics in the short-time regime.^{1,12–22}

Previously reported optical heterodyne-detected optical Kerr effect (OHD-OKE) experiments on time scales from a few hundred femtoseconds to $\sim 1 \mu\text{s}$ revealed power-law decays at short times and the LdG exponential decay at long times.^{1,18–21} The OHD-OKE experiment measures the time derivative of the polarizability-polarizability correlation function,^{23–26} which is equivalent to the orientational correlation function except on < 1 ps time scales where there may be collision-induced contributions. The data were fit for times > 2 ps with a phenomenological fitting function consisting of two power laws times an exponential decay reflecting the LdG decay.^{18–20} This phenomenological fitting function was identical in form to the function used to describe the orientational relaxation dynamics measured with OHD-OKE experiments on supercooled liquids.¹ It was shown that five supercooled liquids and four nematogens in the isotropic phase displayed the identical functional form of the experimental decays over a wide range of times and of temperatures, although the values of the exponents in the power laws are different for the two classes of fluids.¹

In this paper OKE data on two additional nematogens, 4-(trans-4'-n-octylcyclohexyl)isothiocyanatobenzene (8-CHBT), and 4-(4'-pentyl-cyclohexyl)-benzotrile (5-PCH) are presented along with experimental results on one of the previously reported nematogens 4'-pentyl-4-biphenyl-carbonitrile (5-CB). The new data on 8-CHBT and 5-PCH display the same time and temperature-dependent behavior as found for the four previously studied nematogens. This behavior is briefly reviewed. A schematic mode coupling theory is presented and shown to be capable of reproducing the data. The agreement between theory and experiment is excellent from very short times (~ 500 fs) through the LdG decay (hundreds of nanoseconds) over a wide range of temperatures, from well above the NI transition down to temperatures very close to T_{NI} . The theory is a modification of a recent schematic mode coupling theory that has been used successfully to describe OHD-OKE experiments on supercooled liquids.^{27,28} In the recent schematic MCT model used to describe the OHD-OKE data for supercooled liquids, two correlation functions are involved, one for the density and one for the experimental observable. The correlation function that represents the observable, the orientation (polarizability-polarizability) correlation function, is coupled to the density correlator. This schematic mode coupling theory was able to reproduce experimental data over a wide range of times and temperatures^{27,28} including temperatures below the MCT critical temperature, T_C .²⁸ However, we found that this MCT model could not reproduce the time dependence of the OHD-OKE data on nematogens in the isotropic phase. In addition, it did not display the divergence of the long-time exponential decay time constant (see Fig. 1 below), that is, it is not in accord with the behavior as T^* is approached from above that

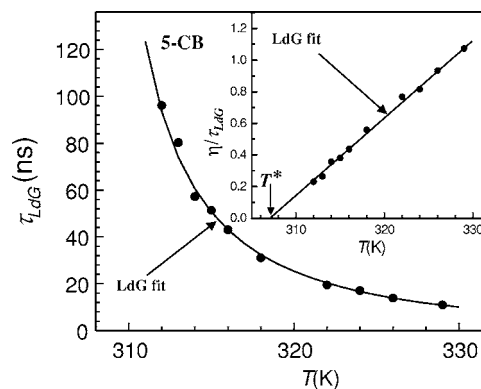


FIG. 1. The temperature dependent Landau-de Gennes relaxation times, τ_{LdG} , for the long time exponential portion of the OHD-OKE 5-CB data vs temperature. The solid line through the points is a fit using the LdG theory, Eq. (2). The inset shows the linear relation predicted by LdG theory.

is successfully described by the LdG theory. The schematic MCT presented below includes additional terms in the orientation correlation function to specifically account for the LdG long-time behavior.

II. THE NEMATOGEN OHD-OKE DATA

OHD-OKE spectroscopy^{29–32} was used to measure the orientational dynamics of the nematogens 8-CHBT, 5-PCH, and previously 5-CB.^{18–20} A sample of the data will be presented below. In the OHD-OKE experiment, a pump pulse creates a time-dependent optical anisotropy that is monitored via a heterodyne detected probe pulse with a variable time delay. The OHD-OKE experiment measures the time derivative of the polarizability-polarizability (orientational) correlation function. The Fourier transform of the OHD-OKE signal is directly related to data obtained from depolarized light scattering,^{23–26,33} but the time domain OHD-OKE experiment can provide a better signal-to-noise ratio over a broader range of times for experiments conducted on very fast to moderate time scales.

To observe the full range of the dynamics several sets of experiments were performed with different pulse lengths and delays. For times $t < 30$ ns, a mode-locked 5 kHz Ti:Sapphire laser/regenerative amplifier system was used ($\lambda = 800$ nm) for both pump and probe. As has been described in detail previously, the pulse length was adjusted from 100 fs to 100 ps as the time scale of the measurement increased to improve the signal-to-noise ratio. The longer pulses produce a greater amplitude signal for the longer time portions of the data. The shortest pulses were used for times 100 fs to a few tens of picoseconds. For longer times, a few picoseconds to 600 ps, the pulses were lengthened to 1 ps. For intermediate times, a 100 ps pulse was used with a long delay line to obtain data from 100 ps to 30 ns. For even longer times, a cw diode laser was used as the probe, and a fast digitizer (1 ns per point) recorded the data. The scans taken over various time ranges overlapped substantially, permitting the data sets to be merged by adjusting only their relative amplitudes. Additional experimental details have been published.^{19,34}

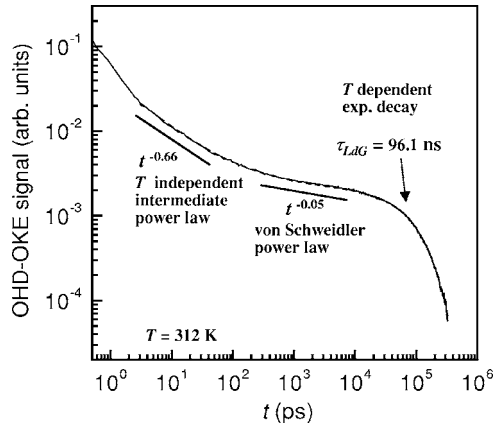


FIG. 2. OHD-OKE 5-CB data in the isotropic phase displayed on a log plot. A fit to the data using the phenomenological fitting function, Eq. (3), is also shown for $t > 2$ ps. The longest time component is an exponential decay described by the Landau-de Gennes theory with a decay constant of 96 ns. Prior to the exponential decay is the von Schweidler power law, $t^{-0.05}$. At shorter time ($> \sim 3$ ps) is the intermediate power law. The lines below the data are aids to the eyes. The very short time decay (< 3 ps) is not described by Eq. (3).

The nematogens were purchased from Aldrich and used without further purification except for filtration through a $0.2 \mu\text{m}$ disk filter to reduce scattered light. The samples were sealed under vacuum in 1 cm glass cuvettes. The cuvettes were held in a constant flow cryostat where the temperature was controlled to ± 0.1 K.

As an example of the efficacy of the LdG theory for the long time scale orientational relaxation of nematogens in the isotropic phase, OHD-OKE data for 5-CB are shown in Fig. 1.¹⁸ The decays are exponential and the decay time constant, τ_{LdG} , is given by

$$\tau_{\text{LdG}} = \frac{V_{\text{eff}} \eta(T)}{k_B(T - T^*)}, \quad (2)$$

where V_{eff} is the effective volume of the nematogen, $\eta(T)$ is the temperature dependent viscosity, and k_B is Boltzmann's constant. The main body of Fig. 1 shows a plot of τ_{LdG} vs T . The solid line through the data points is obtained from Eq. (2) using V_{eff} and T^* as fitting parameters and literature values of the viscosity.³⁵ The inset shows a plot of η/τ_{LdG} vs T . As predicted by the LdG theory, the points should fall on a line and extrapolate to T^* .

Figure 2 displays OHD-OKE data of 5-CB at 312 K on a log plot over a full range of times covering approximately six decades.¹⁸ For $t > \sim 10$ ns, the data decay as a single exponential as described by the LdG theory. However, at shorter times, the data are nonexponential. Just prior to the LdG exponential decay is a power-law decay. At still shorter times there is another power-law decay, and for times less than ~ 2 ps there is a steep rise. Employing the terminology used to describe the analogous decays found for supercooled liquids,^{28,31,32} the short-time power law is called the intermediate power law and the longer-time power law is the von Schweidler power law.^{1,20,31,36} These short-time nonexponential portions of the decay are not described by LdG theory. The form of the data for $t \geq 2$ ps can be described by the phenomenological function^{1,21,32}

$$F(t) = [pt^{-1+c} + dt^{b-1}] \exp(-t/\tau_{\text{LdG}}). \quad (3)$$

The OHD-OKE data are the derivative of the correlation function. c and b are the exponents in the correlation function. The dashed line through the data, which is difficult to discern, is the fit to the data using Eq. (3) for $t > 2$ ps. It was found that six nematogens and five supercooled liquids studied all have this same functional form.^{1,37} (For supercooled liquid systems the decay constant of the exponential decay is called τ_α , because the longest time scale relaxation is called the α -relaxation^{30,36}) However, the exponents c and b are different for supercooled liquids and the nematogens.²⁰

The comparison between OHD-OKE data taken on supercooled liquids and on nematogens in the isotropic phase shows that there are striking similarities but with some major and systematic differences. Recently, OHD-OKE data on supercooled liquids has been reproduced by a schematic mode coupling theory model over a wide range of times and temperatures.^{27,28} The MCT model was able to reproduce the appearance of the boson peak at and below T_C .²⁸ However, it was found that this same model could not accurately reproduce the time and temperature dependence of the nematogen data. The similarities in the supercooled liquid data and the nematogen isotropic phase data suggest the possibility that a modified version of the successful MCT model might be found that would properly describe the nematogen data.

III. SCHEMATIC MCT MODEL FOR NEMATOGENS IN THE ISOTROPIC PHASE

The characteristics of the experimental data suggest that a comprehensive theory should contain the physics of Landau-de Gennes theory for the long-time relaxation and that of schematic models of mode coupling theory for intermediate and short-time relaxation. In the following discussion, we show that it is possible to formulate a schematic model that combines these two. The derivation below is heuristic and represents an educated guess about the structure of a schematic model that might ultimately be derivable from a more rigorous fundamental theory.

Let $\Phi(t)$ be the autocorrelation function of the anisotropy of the polarizability. Its time derivative is directly related to the observable in the experiment. A very general form for the kinetic equation of this autocorrelation function is the following memory function equation,

$$\dot{\Phi}(t) = - \int_0^t dt' M(t-t') \Phi(t'), \quad (4)$$

where $M(t)$ is the memory function associated with $\Phi(t)$.

A schematic mode coupling model for the memory function (such as the Götze-Sperl theory²⁷ for OKE susceptibilities of molecular liquids, the work of Franosch *et al.*³⁸ for light scattering, and the model of Sjögren³⁹ for the diffusion of impurities in a dense fluid) expresses the memory function as

$$M_{\text{MCT}}(t) = \Omega^2 K(t), \quad (5)$$

where Ω is the characteristic frequency, $K(0)=1$, and the time dependence of $K(t)$ is expressed in terms of its memory

function $m(t)$ in the following way.

$$\dot{K}(t) = -\mu K(t) - \Omega^2 \int_0^t dt' m(t-t') K(t'), \quad (6)$$

where μ is the damping constant. The standard assumption about $m(t)$ in schematic mode coupling theory is

$$m(t) = \kappa \Phi(t) \phi_1(t), \quad (7)$$

where k is the coupling constant and $\phi_1(t)$ is the solution of an F_{12} schematic model for what is usually referred to as the density correlator. These equations define the customary schematic mode coupling theory for the autocorrelation function of an observable that is coupled to a mode coupling transition.

The Landau-de Gennes theory of the isotropic-nematic transition describes the relaxation of the order parameter for molecular orientations on a long time scale. It is reasonable to assume that the anisotropy of the polarizability is proportional to (at least for long times or low frequencies) the order parameter that is calculated in Landau-de Gennes theory. For small fluctuations at equilibrium, at temperatures above that of the isotropic-nematic transition, the theory predicts exponential decay of the correlation function as discussed above.

$$\dot{\Phi}(t) = -\Gamma \Phi(t). \quad (8)$$

The relaxation time $\Gamma^{-1} (\Gamma^{-1} = \tau_{\text{LdG}})$ diverges as $(T - T^*)^{-1}$ as the critical temperature T^* of the isotropic-nematic transition is approached from above. Equation (8) is of the form of the very general Eq. (4), where the memory function is of the form

$$M_{\text{LdG}}(t) = \Gamma \delta(t). \quad (9)$$

Other formulas, with more slowly varying functions replacing the Dirac delta function are possible, but given the slow decay of the correlation function, use of the Dirac delta function is adequate for our purposes here.

A simple way to get a combined theory is just to assume that the total memory function of the correlator of interest is the sum of the mode coupling memory function and the Landau-de Gennes memory function.

$$M(t) = M_{\text{MCT}}(t) + M_{\text{LdG}}(t). \quad (10)$$

This is a conjecture, but it is reasonable because the two theories describe very different effects that dominate on different time scales.

The conjecture leads to the following sets of differential equations. To make the notation similar to what has been used previously, replace $\Phi(t)$ by $\phi_2(t)$, $K(t)$ by $K_2(t)$, Ω by $\Omega_2(t)$, μ by μ_2 , and m by $m_2(t)$.

Equations for the measurable correlation function $\phi_2(t)$:

$$\dot{\phi}_2(t) = -\Gamma \phi_2(t) - \Omega_2^2 \int_0^t dt' K_2(t-t') \phi_2(t'),$$

$$\dot{K}_2(t) = -\mu_2 K_2(t) - \Omega_2^2 \int_0^t dt' m_2(t-t') K_2(t'), \quad (11)$$

$$m_2(t) = \kappa \phi_2(t) \phi_1(t).$$

The initial conditions are $\phi_2(0)=1$ and $K_2(0)=1$. Equations for the density correlation function $\phi_1(t)$:

$$\dot{\phi}_1(t) = -\Omega_1^2 \int_0^t dt' K_1(t-t') \phi_1(t'),$$

$$\dot{K}_1(t) = -\mu_1 K_1(t) - \Omega_1^2 \int_0^t dt' m_1(t-t') K_1(t'), \quad (12)$$

$$m_1(t) = \nu_1 \phi_1(t) + \nu_2 \phi_1(t)^2,$$

where ν_1 and ν_2 are the coupling constants in the memory kernel for density correlator. The initial conditions are $\phi_1(0)=1$ and $K_1(0)=1$. These equations can be recast as second-order differential equations.

$$\ddot{\phi}_1(t) = -\Omega_1^2 \phi_1(t) - \mu_1 \dot{\phi}_1(t) - \Omega_1^2 \int_0^t dt' m_1(t-t') \dot{\phi}_1(t). \quad (13)$$

The initial conditions are $\phi_1(0)=1$ and $\dot{\phi}_1(0)=0$.

$$\begin{aligned} \ddot{\phi}_2(t) = & -(\Omega_2^2 + \mu_2 \Gamma) \phi_2(t) - (\mu_2 + \Gamma) \dot{\phi}_2(t) \\ & - \Omega_2^2 \int_0^t dt' m_2(t-t') \dot{\phi}_2(t') \\ & - \Omega_2^2 \Gamma \int_0^t dt' m_2(t-t') \phi_2(t'). \end{aligned} \quad (14)$$

The initial conditions are $\phi_2(0)=1$ and $\dot{\phi}_2(0)=-\Gamma$.

Calculations employing Eqs. (13) and (14) will be used in the next section to fit temperature dependent OHD-OKE data on nematogens. Equation (13) is identical to the one used in the analysis of supercooled liquid data. The differences between this schematic model and the one applied to supercooled liquids are in Eq. (14). If Γ is set equal to 0 in Eq. (14) [or Eq. (11)], the supercooled liquid model is recovered. Equation (14) is the orientational correlation function coupled to the density correlation function with specific new terms that account for the long-time portion of the data that has previously been described by the LdG theory.

IV. COMPARISON OF THE SCHEMATIC MCT MODEL FOR NEMATOGENS TO DATA

Here the theoretical results presented in the last section will be compared to temperature-dependent OHE-OKE data for nematogens in the isotropic phase. The data were fit using a downhill simplex algorithm. The calculated curves are the time derivative of $\phi_2(t)$ obtained from the joint solution of Eqs. (13) and (14). There are a large number of parameters

in these equations. In the absence of the memory terms, each equation is the equation for a damped harmonic oscillator with frequencies Ω_1 and Ω_2 , and the associated damping constants μ_1 and μ_2 . ν_1 and ν_2 are the amplitudes in the memory kernel m_1 for the F_{12} model that describes the density, and κ is the coupling constant that reflects the strength of the coupling between the orientational correlation function, ϕ_2 , and the density correlation function, ϕ_1 . In addition there is the LdG decay constant, Γ with $\Gamma^{-1} = \tau_{\text{LdG}}$ with τ_{LdG} given in Eq. (2).

To limit the number of parameters in the fitting, a variety of tests were performed to determine the sensitivity of the fits to various parameters. As can be seen in Fig. 2, the exponential decay can be observed for many factors of e . Letting Γ float in a fit to the full time dependence produced virtually the identical Γ values as were found if only the very long-time portion of the curves were fit with a single exponential decay. The variations were not systematic. Therefore, the Γ value at each temperature was found by single exponential fits, and in all of the other fitting, these Γ values were fixed.

For supercooled liquids it has been argued that the oscillator frequency Ω should be in the terahertz range.⁴⁰ We assume that the same is true for Ω_1 and Ω_2 . We have fit the data with many fixed values of Ω_1 adjusting all the other parameters (except for Γ), and found that if the frequency is too low the data cannot be fit. The same is true of Ω_2 . However, within a wide range of terahertz frequencies, the final quality of the fits is unchanged if Ω_1 and Ω_2 are fixed at temperature-independent values and all the other parameters are adjusted at each temperature. Therefore, we have used $\Omega_1 = \Omega_2 = 2$ THz. The values of Ω_1 and Ω_2 do not have to be equal, but the value of Ω_1 determines the value of μ_1 , and the value of Ω_2 determines the value of μ_2 . The first example given below is 5-CB. In preliminary fits of the data for 5-CB, we found that the parameters ν_1 and ν_2 in the memory function of the density correlator and the damping constant μ_1 are virtually independent of temperature. The small variations with temperature did not influence the trends for μ_2 and κ . Therefore, in the final fits, ν_1 , ν_2 , and μ_1 were fixed at temperature-independent values obtained from the average results of the preliminary fits. The coupling term κ and the damping constant for orientation μ_2 were found to be smooth functions of temperature. The results of variation of κ and μ_2 with temperature will be presented and discussed later in this section. For 5-CB $\nu_1 = 0.60$ THz, $\nu_2 = 0.98$ THz, and $\mu_1 = 15.6$ THz.

With Γ , Ω_1 , Ω_2 , ν_1 , ν_2 , and μ_1 fixed, as discussed above, there are only two parameters, μ_2 and κ , that were adjusted at each temperature. Figure 3 displays temperature-dependent data and calculations for 5-CB using the parameters given above and adjusting the parameters, μ_2 and κ at each temperature. The data sets have been offset along the vertical axis for clarity. The fits start from 500 fs. OHD-OKE data for times shorter than 500 fs are not considered because they are obscured by the signal produced by the electronic polarizability of the sample, which is so strong that even with short pulses it overwhelms all other contributions to the signal. The electronic polarizability signal becomes negli-

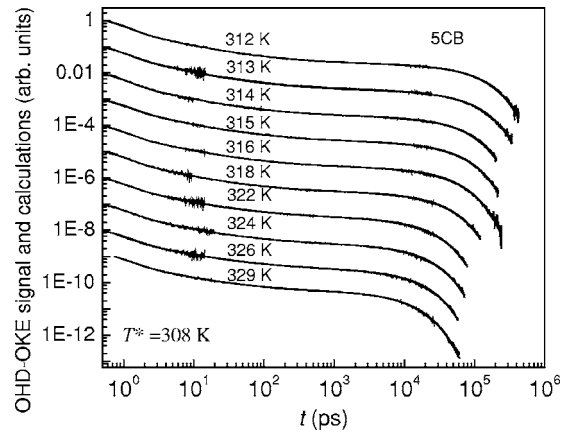


FIG. 3. The temperature-dependent 5-CB OHD-OKE data and the calculated curves using the solution to Eqs. (13) and (14). The curves have been offset along the vertical axis for clarity. The agreement between the calculations and data is excellent on all time scales and temperatures. The MCT curves are calculated for $\Omega_1 = \Omega_2 = 2$ THz, $\nu_1 = 0.60$ THz, $\nu_2 = 0.98$ THz, and $\mu_1 = 15.6$ THz, and using κ and μ_2 as adjustable parameters. The fitting results for κ and μ_2 are given in Figs. 7 and 8.

gible for $t \geq 500$ fs. Over six decades of time window (500 fs to several hundred nanoseconds) and for all the temperatures, the calculated curves fit the data nearly perfectly.

In the previously published work on the liquid-crystal data the very short time portion of the data ($< \sim 3$ ps) is not reproduced using the phenomenological function, Eq. (3).¹ The decay at the very short times is much steeper than the intermediate power law as can be clearly seen in Fig. 2. In more recent studies on liquid crystals,³⁷ the very short time behavior was modeled phenomenologically as a third power law, t^{-s} . The t^{-s} term was added to Eq. (3) in the square bracket along with the intermediate power law and the von Schweidler power law. The modified Eq. (3) was able to describe the liquid-crystal dynamics in the full time window. The exponent s was found to vary somewhat with temperature and fall between 1.5 and 2.5. However, the time window over which the very short time portion of the data can be observed is insufficient to determine its functional form. In MCT of supercooled liquids, the very short time portion of the decay is a power law called the fast β process.^{30,36} Figure 4 displays the 5-CB data at two temperatures on expanded time and amplitude scales along with the same fits that are shown in Fig. 3. The data sets have been offset along the vertical axis for clarity. It is clear from the figure that the schematic MCT model presented in Sec. III does an excellent job of reproducing the data even at the shortest observable times. The quality of the fits at very short times is the same at all temperatures and for the other samples discussed below.

To further test the model, two additional nematogens, 8-CHBT and 5-PCH, were studied in the isotropic phase. The fitting procedures are identical to those described above for 5-CB. The two microscopic frequencies Ω_1 and Ω_2 are fixed to be 2 THz. The LdG decay constant Γ is fixed to τ_{LdG}^{-1} , with τ_{LdG} found by a single exponential fit to the long-time portion of the data at each temperature. The density memory vertices ν_1 and ν_2 , and the density damping constant μ_1 are also fixed, i.e., $\nu_1 = 0.60$, and $\nu_2 = 1.0$ for both samples, and

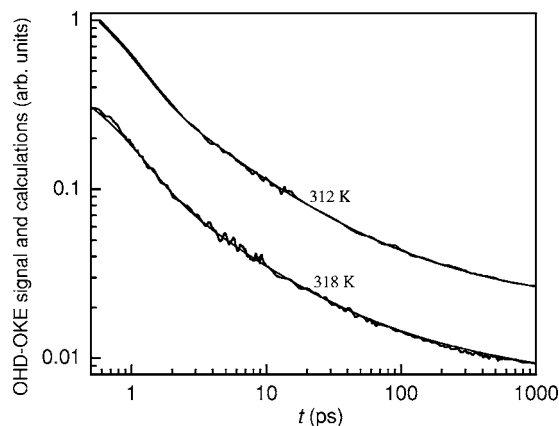


FIG. 4. Two of the data curves and fits shown in Fig. 3 with expanded time scale to emphasize the short time portion of the dynamics. The agreement between the data and calculations holds from the shortest times that could be measured in the experiments.

$\mu_1=20.0$ THz for 8-CHBT and $\mu_1=27.8$ THz for 5-PCH. Figures 5 and 6 display temperature-dependent data and calculations for 8-CHBT and 5-PCH, respectively, using the parameters given above and adjusting the parameters, μ_2 and κ at each temperature. The data sets have been offset along the vertical axis for clarity. The calculated curves coincide with the data so well that they are hardly discernible from the data.

As discussed above, the data for the three liquid crystals were fit by adjusting the translation-rotation coupling coefficient κ and the orientational damping coefficient μ_2 at each temperature. κ is found to increase rapidly as T is decreased toward T^* . Plots of $1/\kappa$ versus the temperature, T , are shown in Fig. 7. Also included in the figure are the linear fits shown as the solid lines through the data points. The error bars are approximately the size of the squares in the figure. The intercepts at the abscissa indicate the temperatures at which κ goes to infinity. It is remarkable that, within experimental error, the translation-rotation coupling, κ , diverges at the same temperature as T^* , where the LdG correlation length ξ

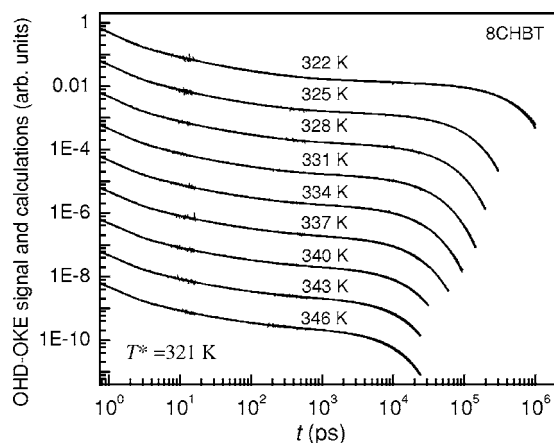


FIG. 5. The temperature-dependent 8-CHBT OHD-OKE data and calculated curves using the solutions to Eqs. (13) and (14). The curves have been offset along the vertical axis for clarity. The MCT curves are calculated for $\Omega_1=\Omega_2=2$ THz, $\nu_1=0.60$ THz, $\nu_2=1.0$ THz, and $\mu_1=20.0$ THz, and using κ and μ_2 as adjustable parameters. The fitting results for κ and μ_2 are given in Figs. 7 and 8.

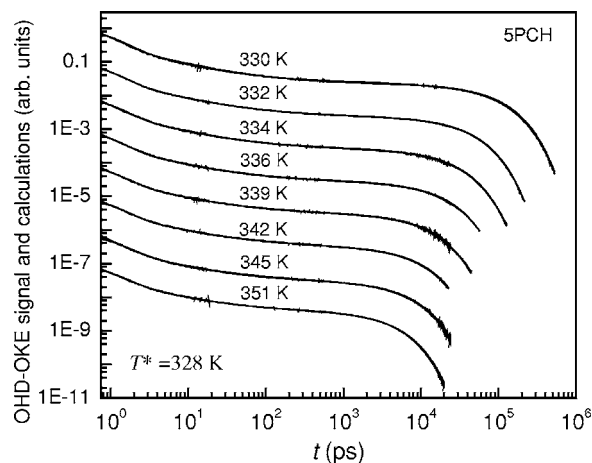


FIG. 6. The temperature-dependent 5-PCH OHD-OKE data and the calculated curves using the solutions to Eqs. (13) and (14). The curves have been offset along the vertical axis for clarity. The MCT curves are calculated for $\Omega_1=\Omega_2=2$ THz, $\nu_1=0.60$ THz, $\nu_2=1.0$ THz, and $\mu_1=27.8$ THz, and using κ and μ_2 as adjustable parameters. The resulted values for κ and μ_2 are given in Figs. 7 and 8.

diverges [Eq. (1)]. An important point to emphasize is that the results presented above for the temperature dependence of κ are independent of the choice of Ω_1 and Ω_2 , and whether other parameters, ν_1 , ν_2 , and μ_1 were fixed or allowed to vary. In a previous schematic MCT analysis of supercooled liquid OHD-OKE data, Götze and Sperl,²⁷ reported that κ followed an Arrhenius law $\exp(T_0/T)$ with $T_0=1000$ K for supercooled salol. When the MCT schematic model of Götze and Sperl,³⁹ Eqs. (4)–(7), was used to de-

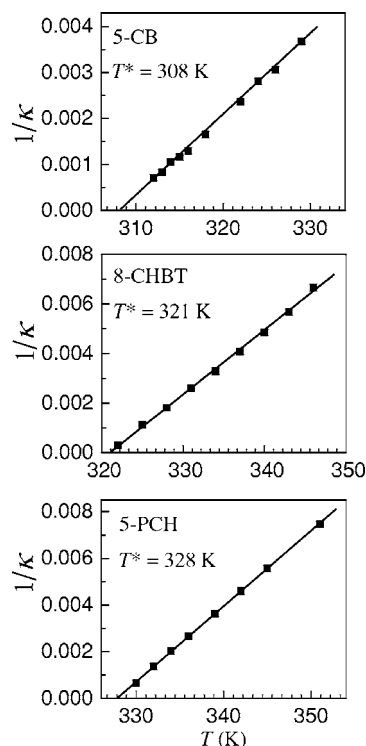


FIG. 7. The temperature dependence of the translation-rotation coupling parameter κ (plotted as $1/\kappa$). The values of κ are obtained from the fits in Figs. 3, 5, and 6. Within experimental error κ diverges at the LdG temperature, T^* .

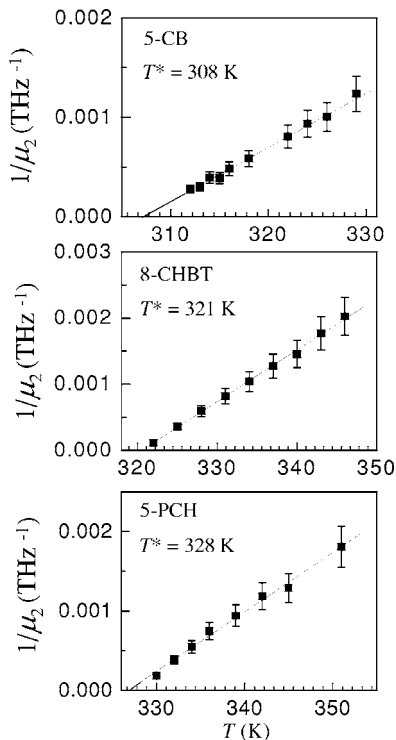


FIG. 8. The temperature dependence of the orientation damping constant μ_2 (plotted as $1/\mu_2$). The values of μ_2 are obtained from the fits in Figs. 3, 5, and 6. Within experimental error μ_2 diverges at the LdG temperature, T^* .

scribe the short time and low-temperature behaviors of supercooled liquid dynamics,²⁸ the results indicated that increasing translation-rotation coupling is responsible for the appearance of the boson peak as the temperature approaches and drops below T_C . However, neither of the studies on supercooled liquids indicated a divergence in κ .

The fact that κ appears to grow without limit as T^* is approached suggests that the divergence is associated with the diverging orientational correlation length in the isotropic phase as the isotropic-nematic transition is approached. Schematic mode coupling models represent simple mathematical models for more complete kinetic theories that make the mode coupling approximations. In principle, parameters such as κ in schematic models are related to well-defined parameters in the more detailed kinetic theory. In situations for which these theories have been developed to date (see e.g., Ref. 35), these latter parameters can be expressed in terms of the static correlation functions of the fluid. It would not be at all surprising if the strength of the coupling between translation and rotation in a mode coupling theory for nematogens in the isotropic phase might contain the orientational correlation function that has a diverging correlation length. This is a plausible explanation of the apparent divergence of κ .

The temperature dependences of the orientational damping constants μ_2 for the three nematogens have similar behavior to that of the coupling constant κ . Plots of $1/\mu_2$ vs T , are shown in Fig. 8 with the error bars included. The errors were determined by the values of μ_2 that give worse fits to the data by visual inspection. The points are the center of the error bars. μ_2 increases rapidly and tends to diverge as T

decreases toward the NI transition temperature. However, in contrast to κ , the μ_2 error bars are significant. The straight lines are linear fits to the $1/\mu_2$ values. $1/\mu_2$ diverges as T approaches T^* with the values for the three nematogens almost identically the T^* values found from the LdG analysis. Given the error bars, the fact that the linear fits give almost perfect T^* values may be somewhat fortuitous, but there is no doubt that $1/\mu_2$ is diverging as T^* is approached and the temperatures at which the divergences occur are close to or equal to the T^* values of the three nematogens. In fitting the data with μ_2 as one of the two parameters that were adjusted at each temperature, the very short time portion (<3 ps) was dominant in determining the values. If only data >3 ps is fit, μ_2 could be held constant and good fits could be obtained at all temperatures. In the previous work where the Sjögren model³⁹ was used to describe the OHD-OKE (Ref. 27) and depolarized light scattering³⁸ data on supercooled liquids, the two damping terms μ_1 and μ_2 were fixed or found to be independent of temperature. When the same model was applied to describe the boson peaks observed at short times and low temperatures in OHD-OKE data in supercooled liquids, μ_2 was independent of T and μ_1 was found to be nearly constant above T_c but increased rapidly when the temperature dropped below T_c towards T_g .²⁸ For nematogens in the isotropic phase, when using the schematic MCT model for nematogens presented here, μ_1 is independent of T , and μ_2 diverges as T approaches the LdG temperature T^* .

V. CONCLUDING REMARKS

We have presented OHD-OKE data on the nematogens 8-CHBT and 5-PCH in their isotropic phases and have analyzed them and previously reported 5-CB data using a new schematic MCT model based on the model that has been successfully applied to the analysis of supercooled liquid data.^{27,28} The same MCT analysis was applied to the other three liquid crystals that have been studied with OHD-OKE experiments with analogous results. The current model is based on the Sjögren model,³⁹ with additional terms tailored specifically for nematogens in the isotropic phase. This schematic nematogen MCT model was shown to do an outstanding job of reproducing the temperature-dependent OHD-OKE data over approximately six decades of time from very short times <1 ps to the longest time scale of the LdG exponential decay. The divergence of the parameters κ , the orientational to density coupling parameter, and μ_2 , the orientational damping parameter at T^* may suggest a fruitful avenue of investigation to obtain a physical understanding of the connection between the current model and LdG theory.

The additional terms included in the nematogen MCT model do more than reproducing the LdG temperature dependence of the final exponential decay. The standard MCT approach, which works well for supercooled liquids, is not able to reproduce the von Schweidler power law exponents [b in Eq. (3)], which are very close to 1 for the nematogens, and also reproduce the rest of the curve. The LdG theory provides a well-defined physical basis for the isotropic to nematic phase transition³ However, it does not provide any description of nematogen dynamics on time scales shorter

than the time for the randomization of the pseudonematic domains. The schematic nematogen MCT model presented here incorporates aspects of the LdG description, and it is able to reproduce the full orientational time dependence of nematogens in their isotropic phase.

The time dependence of the orientational correlation function obtained from our schematic mode coupling model, for times earlier than the long time exponential decay, is determined by the coupling of the orientational correlation function to an F_{12} schematic model for what is normally referred to as a density correlator. In fact, the F_{12} model is a representation of the correlation function for a variable that relaxes very slowly near the mode coupling transition. For a molecular liquid, it presumably is a correlator for a “density” of orientational degrees of freedom as well as center-of-mass degrees of freedom, but a detailed understanding of the meaning of that correlator cannot be obtained from the present experiments. Under the conditions of the experiments discussed here, the temperatures are well above any mode coupling transition. The fact that the theory discussed here fits the experimental data so well suggests that, for times less than the long exponential decay time, the time dependence of the orientational correlator of these nematogens in the isotropic phase is determined by mode coupling effects. However, the nature of the mode to which the orientational correlation function is coupled cannot be determined from the data. The mathematical features of a correlation function that results from such coupling are the essential predictions of schematic mode coupling theory. These mathematical features are independent of the physical nature of the unknown mode, but it is clear from the comparisons between data calculations presented here that the experimental data has these mathematical features.⁴¹

ACKNOWLEDGMENTS

The work of the authors (J.L.), (H.C.), and (M.D.F) was supported by the NSF through Grant No. DMR-0332692. The work of one of the authors (H.C.A.) was supported by the NSF through Grant No. CHE-0408786.

¹H. Cang, J. Li, V. N. Novikov, and M. D. Fayer, *J. Chem. Phys.* **118**, 9303 (2003).

²P. G. de Gennes, *Phys. Lett.* **28**, 725 (1969).

³P. G. de Gennes, *The Physics of Liquid Crystals* (Clarendon, Oxford, 1974).

⁴G. K. L. Wong and Y. R. Shen, *Phys. Rev. Lett.* **30**, 895 (1973).

⁵E. G. Hanson, Y. R. Shen, and G. K. L. Wong, *Phys. Rev. A* **14**, 1281 (1976).

⁶T. D. Gierke and W. H. Flygare, *J. Chem. Phys.* **61**, 2231 (1974).

⁷T. W. Stinson III and J. D. Litster, *Phys. Rev. Lett.* **25**, 503 (1970).

⁸J. D. Litster and T. W. Stinson III, *J. Appl. Phys.* **41**, 996 (1970).

⁹J. C. Fillippini and Y. Poggi, *Phys. Lett.* **65**, 30 (1978).

¹⁰W. H. de Jeu, in *Solid State Physics*, edited by L. Liebert (Academic, New York, 1978), pp. 109.

¹¹H. Kresse, in *Advances in Liquid Crystals*, edited by G. H. Brown (Academic, New York, 1983), Vol. 6, pp. 109.

¹²J. J. Stankus, R. Torre, C. D. Marshall, S. R. Greenfield, A. Sengupta, A. Tokmakoff, and M. D. Fayer, *Chem. Phys. Lett.* **194**, 213 (1992).

¹³J. J. Stankus, R. Torre, and M. D. Fayer, *J. Phys. Chem.* **97**, 9478 (1993).

¹⁴F. W. Deeg, S. R. Greenfield, J. J. Stankus, V. J. Newell, and M. D. Fayer, *J. Chem. Phys.* **93**, 3503 (1990).

¹⁵R. Torre and S. Califano, *J. Chim. Phys. Phys.-Chim. Biol.* **93**, 1843 (1996).

¹⁶R. Torre, F. Tempestini, P. Bartolini, and R. Righini, *Philos. Mag. B* **77**, 645 (1998).

¹⁷R. S. Miller and R. A. MacPhail, *Chem. Phys. Lett.* **241**, 121 (1995).

¹⁸S. D. Gottke, H. Cang, B. Bagchi, and M. D. Fayer, *J. Chem. Phys.* **116**, 6339 (2002).

¹⁹S. D. Gottke, D. D. Brace, H. Cang, B. Bagchi, and M. D. Fayer, *J. Chem. Phys.* **116**, 360 (2002).

²⁰H. Cang, J. Li, and M. D. Fayer, *Chem. Phys. Lett.* **366**, 82 (2002).

²¹H. Cang, J. Li, V. N. Novikov, and M. D. Fayer, *J. Chem. Phys.* **119**, 10421 (2003).

²²D. Chakrabarti, P. P. Jose, S. Chakrabarty, and B. Bagchi, *Phys. Rev. Lett.* **95**, 197801 (2005).

²³Y. X. Yan, L. G. Cheng, and K. A. Nelson, *Adv. Infrared Raman Spectrosc.* **16**, 299 (1987).

²⁴Y. X. Yan and K. A. Nelson, *J. Chem. Phys.* **87**, 6240 (1987).

²⁵Y. X. Yan and K. A. Nelson, *J. Chem. Phys.* **87**, 6257 (1987).

²⁶F. W. Deeg, J. J. Stankus, S. R. Greenfield, V. J. Newell, and M. D. Fayer, *J. Chem. Phys.* **90**, 6893 (1989).

²⁷W. Götze and M. Sperl, *Phys. Rev. Lett.* **92**, 105701 (2004).

²⁸H. Cang, J. Li, H. C. Andersen, and M. D. Fayer, *J. Chem. Phys.* **123**, 064508 (2005).

²⁹D. McMorro, W. T. Lotshaw, and G. A. Kenney-Wallace, *IEEE J. Quantum Electron.* **24**, 443 (1988).

³⁰G. Hinze, D. D. Brace, S. D. Gottke, and M. D. Fayer, *J. Chem. Phys.* **113**, 3723 (2000).

³¹H. Cang, V. N. Novikov, and M. D. Fayer, *Phys. Rev. Lett.* **90**, 197401 (2003).

³²H. Cang, V. N. Novikov, and M. D. Fayer, *J. Chem. Phys.* **118**, 2800 (2003).

³³Y. Kai, S. Kinoshita, M. Yamaguchi, and T. Yagi, *J. Mol. Liq.* **65–6**, 413 (1995).

³⁴S. D. Gottke, D. D. Brace, G. Hinze, and M. D. Fayer, *J. Phys. Chem. B* **105**, 238 (2001).

³⁵J. Jadzyn, R. Dabrowski, T. Lech, and G. Czenchowski, *J. Chem. Eng. Data* **46**, 110 (2001).

³⁶W. Götze, *Liquids, Freezing and Glass Transition*. (Elsevier, Amsterdam, 1989).

³⁷J. Li, I. Wang, and M. D. Fayer, *J. Chem. Phys.* (to be published) (2005).

³⁸T. Franosch, W. Götze, M. R. Mayr, and A. P. Singh, *Phys. Rev. E* **55**, 3183 (1997).

³⁹L. Sjögren, *Phys. Rev. A* **33**, 1254 (1986).

⁴⁰P. Boon and S. Yip, *Molecular Hydrodynamics* (McGraw-Hill, New York, 1980).

⁴¹When this manuscript was being modified after initial review, we received a preprint of a paper by Chakrabarti *et al.* (Ref. 22) This paper proposes a physical mechanism to explain the short-time behavior of the orientational correlation function. Large fluctuations of the orientational order parameter near the isotropic-nematic transition can lead to power-law decay at short to intermediate times. A preliminary theory of this effect, which takes into account fluctuations within the isotropic phase near the transition, was presented by Gottke *et al.* (Ref. 19) The resulting approximate expression for the short time behavior of the correlation function [Eq. (22) of Ref. 19 or Eq. (5) of Ref. 22] does not give a satisfactory fit to the experimental data in the present paper. Chakrabarti *et al.* (Ref. 22) have noted that near the transition there is also the possibility of order parameter fluctuations that result from fluctuations between the isotropic and nematic phases. A full theory of this effect has not been presented and hence cannot be compared with experiment at this time.